Influence of Molecular Structure on Double Ionization of N_2 and O_2 by High Intensity Ultrashort Laser Pulses

E. Eremina,[1] X. Liu,[1] H. Rottke,[1] W. Sandner,[1] M. G. Schätzel,[2] A. Dreischuh,[2,3] G. G. Paulus,[2,4,5] H. Walther,[2,4]
R. Moshammer,[6] and J. Ullrich[6]
[1]*Max-Born-Institut, Max-Born-Strasse 2a, 12489 Berlin, Germany*
[2]*Max-Planck-Institut für Quantenoptik, Hans-Kopfermann-Strasse 1, 85748 Garching, Germany*
[3]*Department of Quantum Electronics, Sofia University, 5 James Bourchier Boulevard, 1164 Sofia, Bulgaria*
[4]*Ludwig-Maximilians-Universität München, Am Coulombwall 1, 85748 Garching, Germany*
[5]*Department of Physics, Texas A&M University, College Station, Texas 77843-4242, USA*
[6]*Max-Planck-Institut für Kernphysik, Saupfercheckweg 1, 69117 Heidelberg, Germany*
(Received 4 September 2003; published 26 April 2004)

The electron momentum correlation after nonsequential double ionization of N_2 and O_2 in ultrashort light pulses at light intensities near 1.5×10^{14} W/cm^2 has been investigated. The experimental results reveal distinctive differences between the molecular species and between molecules and atoms of similar ionization threshold. We provide evidence that recollision double ionization is the essential mechanism and trace the origin of the differences back to the symmetry of the orbitals occupied by the valence electrons.

DOI: 10.1103/PhysRevLett.92.173001 PACS numbers: 33.80.Rv, 33.80.Wz

Single ionization of atoms as well as molecules in high intensity ultrashort light pulses and the closely related high order harmonic generation (HHG) has been found to be precisely describable within a single active electron model. Only the electron which is ionized has to be taken into account; no evidence of electron-electron correlation on the final outcome of HHG and ionization has been found in experimental data. The situation is completely different for double and multiple ionization. Indeed, at moderate light intensity these processes are driven by correlation between electrons. The first signature of its presence was found in unexpectedly high double ionization probabilities which were inconsistent with sequential ionization [1]. Further investigations have shown that inelastic electron-electron scattering [2] driven by the oscillating electric field of the light pulse plays a decisive role for nonsequential double ionization (NSDI) of atoms [3–7]. NSDI starts with the release of one electron via electric field ionization. It is subsequently accelerated by the electric field of the light pulse. Under certain conditions, it revisits the ion core within the same optical cycle with a considerable kinetic energy E_{kin} which can exceed the photon energy by more than an order of magnitude. Depending on E_{kin}, an inelastic collision can either result in instantaneous impact ionization or in electronic excitation of the ion. The excited electron then can easily be removed by electric field ionization [7].

Similar to atoms, simple two-atomic molecules such as N_2 and O_2 also show an excessive double ionization probability indicative of NSDI [8–11]. However, the *total* ion-yield data are not sufficient to identify the mechanism. The presence of revisiting electrons, which are at the basis of atomic NSDI, was recently reported for molecular hydrogen [12,13]. Thus, one may expect that electron correlation in a rescattering event is also at the basis of molecular NSDI in general.

In this Letter, we investigate double ionization of N_2 and O_2 *differentially* in order to identify the nonsequential mechanism and to investigate molecule specific effects on the final electron momentum correlation. Single ionization experiments have shown that these molecules have a distinctly different behavior. With respect to total ion yield as a function of intensity [9] and electron kinetic energy spectra [14], N_2 behaves similar to the noble gas atom Ar which has virtually the same ionization potential. On the other hand, O_2 and Xe, also having similar ionization potentials, clearly differ. Ionization of O_2 is suppressed with respect to Xe [9,15] with the photoelectron spectra showing a reduced electron yield at small and high kinetic energies [14]. These effects have been attributed to the different symmetry of the ground state orbitals occupied by the valence electron [N_2: σ_g (bonding); O_2: π_g (antibonding)] [14,16]. Indeed this is able to account for the experimental findings [14,16,17]. We will show that NSDI sensitively depends on the molecular species also. The differential data of O_2 even lack the signatures considered to be characteristic for NSDI. Most surprisingly, however, a simple classical model based on electron recollision double ionization is able to reproduce qualitatively the experimental findings *provided* the symmetry of the initial state orbitals occupied by the valence electrons is taken into account. The experiment selectively investigates the N_2 and O_2 double ionization channel, i.e., only events for which metastable doubly charged molecular ions reach the ion detector are considered. They can be formed only by double ionization in a restricted range of internuclear separations around the equilibrium point [20], thus "freezing" nuclear motion during the laser pulse.

The experimental technique is based on correlated electron and ion momentum spectroscopy [5,21–23]. In short, ions and electrons created in the focal spot of a laser beam at the point of intersection with a supersonic molecular beam are extracted by a weak electric field (1–7 V/cm). Electrons are guided by a suitably chosen homogeneous magnetic field (≈ 10–20 G) parallel to the electric field. After passage of acceleration and field-free drift tubes, the charged particles hit position-sensitive microchannel-plate detectors (diameter 80 mm) equipped with delay line anodes for position encoding. The measured time of flight of each particle together with the position where it strikes the detector allows the reconstruction of its complete initial momentum vector. The solid angle of detection is 4π for ions and electrons.

Correlated detection of ions and electrons is possible only if the probability for an ionization event—be it single or double—is small (≈ 0.1) per laser shot. Together with the small yield ratio for double to single ionization ($\approx 10^{-3}$ for O_2 and $\approx 5 \times 10^{-3}$ for N_2 [24]), this means that an event of interest can be detected only every 10000th laser shot on the average. This calls for a laser system with the highest possible pulse repetition rate while being sufficiently powerful to provide the necessary intensity for NSDI. Our laser system delivers 35 fs pulses (FWHM) with an energy up to 6 μJ/pulse at a central wavelength of 800 nm [25]. The repetition rate is 100 kHz which is unique in this type of experiment. The laser beam is focused by a parabolic mirror ($f = 80$ mm) on the atomic beam which has a width of 50 μm along the propagation direction of the laser beam. This gives rise to an interaction volume of $\approx 2 \times 10^{-9}$ cm^3. The background gas pressure is kept below 3×10^{-10} mbar.

The sum-momentum distribution of the two photoelectrons for the momentum component parallel to the direction of linear laser beam polarization is considered to provide most obviously an indication of the mechanism of NSDI. Figure 1 shows this distribution (connected squares) for N_2 at 1.5×10^{14} W/cm^2 (a), and for O_2 at 1.1×10^{14} W/cm^2 (b) and at 1.7×10^{14} W/cm^2 (c). The laser intensities were chosen in a regime where NSDI has been reported to dominate [9,10]. Both N_2 as well as O_2 do not show the double hump structure considered to be characteristic for NSDI due to recollision. Most clearly, this double hump structure in the sum-momentum distributions was found for Ne [5]. However, also in the present case the "cutoff" [23] for the N_2 distribution is located close to $\pm 4\sqrt{U_p}$ as expected for instantaneous impact ionization of N_2^+ via electron recollision [23] [Fig. 1(a)]. U_p denotes the ponderomotive energy, i.e., the quiver energy of an electron in the laser field. Moreover, the correlation of the final state electron momentum components parallel to the laser beam polarization vector in Fig. 2(a) clearly shows the characteristics expected for recollision double ionization of N_2. Like the atomic case, the two photoelectrons are emitted preferentially with similar momentum components ($p_{i,\parallel}$, $i = 1, 2$) into the same half space [6,7,23,26]. However, different from Ar at the same light intensity [23], significantly more electron pairs are found with small momenta ($p_{i,\parallel} \approx 0$) for both of them, close to the main diagonal of the correlation plot. As will be shown below, these pairs may be attributed to rescattering impact ionization of N_2^+. The final momentum correlation of this NSDI mechanism is thus decisively influenced by the molecular structure. Similar to Ar, those electron pairs in the second and forth quadrants of Fig. 2(a) found significantly off the main diagonal have to be attributed to rescattering electron impact excitation of N_2^+ with subsequent electric field ionization of the excited electron [7].

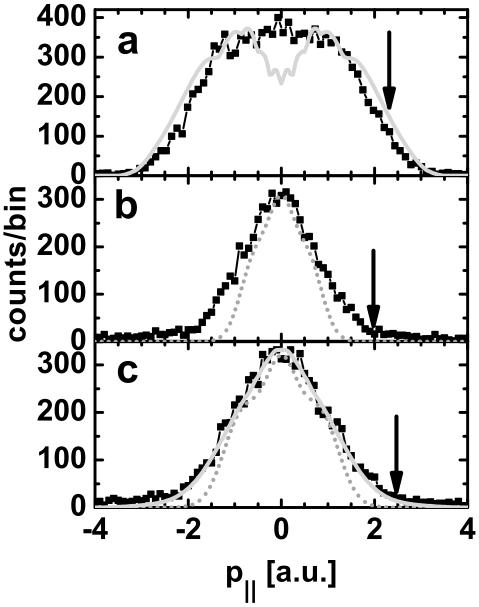

FIG. 1. Measured electron sum-momentum distributions (connected squares) after double ionization of (a) N_2 at 1.5×10^{14} W/cm^2, (b) O_2 at 1.1×10^{14} W/cm^2, and (c) O_2 at 1.7×10^{14} W/cm^2. The distributions are shown projected on an axis parallel to the laser beam polarization vector. The arrows indicate the "cutoff" momentum of $4\sqrt{U_p}$ which is expected for NSDI due to recollision. For O_2, the dotted lines show calculated spectra if sequential double ionization is assumed. The light gray lines in (a) and (c) show the result of our NSDI model.

In contrast, the O_2 sum-momentum distributions [Figs. 1(b) and 1(c)) are much narrower than that for N_2 [Fig. 1(a)], even though the light intensity is higher in Fig. 1(c). The expected cutoff momentum $4\sqrt{U_p}$ is clearly too large. Rather, the observed cutoff is better described by $\pm 2\sqrt{U_p}$. The momentum correlation of the photoelectron pairs in Fig. 2(b) also does not show the characteristics expected for impact ionization in a recollision event. This allows two possible conclusions: Either double ionization proceeds sequentially or the molecular structure modifies the final state momentum correlation of

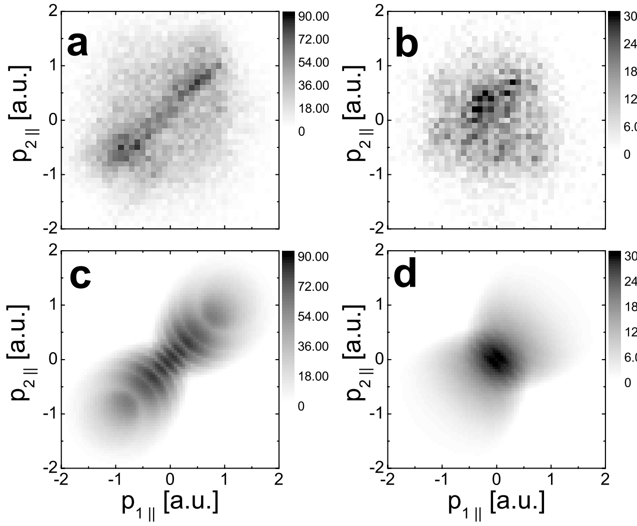

FIG. 2. The measured (a), (b) and corresponding calculated (c), (d) electron momentum correlation for the momentum components parallel to the light beam polarization vector: (a), (c) N_2 at 1.5×10^{14} W/cm^2 and (b), (d) O_2 at 1.7×10^{14} W/cm^2.

NSDI significantly. Total O_2^{++} ion-yield measurements favor the second conclusion [9]. We tested both possibilities. First, we calculated electron sum-momentum distributions expected for sequential ionization using a semiclassical model. Quasistatic electric field ionization is assumed for both ionization steps. The symmetry of the initial state orbitals occupied by the O_2 and O_2^+ valence electrons is included in the calculation, however in a simplified way [27]. Further on, averaging over the randomly oriented internuclear axis was performed because the short light pulses do not align the molecule. The result of the calculation is shown in Figs. 1(b) and 1(c) (dotted lines). Obviously, the theoretical curve is narrower than the experimental one. This result is even more significant as our theoretical model overestimates the width of the momentum distribution. This can be concluded from the comparison of the respective experimental and theoretical results for single ionization. The obvious conclusion is that double ionization does *not* proceed sequentially for O_2 also; i.e., NSDI does exist also for this molecule. The question, however, remains whether recollision is still the underlying mechanism for NSDI of O_2. We address this question by assuming that this *is* the case and compare the experimental data with the results of a theoretical model which includes recollision as well as the symmetry of the initial state of the molecule. In particular, the model should be able to reproduce the completely different sum-momentum distributions and final state electron momentum correlations for O_2 and N_2. The calculation is based on a classical analog of the quantum mechanical S matrix for recollision double ionization [28]. According to this, the differential probability for double ionization $|S(\mathbf{p}_1, \mathbf{p}_2)|^2$ is proportional to a form factor [29]. The form factor here is factorized into a contribution $g_1(\mathbf{k})$ describing the transition of the first electron to the continuum, and another contribution $g_2(\mathbf{p}_1, \mathbf{p}_2, \mathbf{k})$ describing the inelastic recollision. $\mathbf{p}_1$ and $\mathbf{p}_2$ are the final state momenta of the electrons and $\mathbf{k}$ is the intermediate state momentum of the recolliding electron.

The inelastic scattering matrix element g_2 is calculated in Born approximation with the wave function of the bound electron constructed by the method of linear combination of atomic orbitals (LCAO). For the latter, the bound state of a δ potential is used (for justification see [29]). As a consequence, the orbital is either of σ_g or σ_u type. Although the O_2 orbital is not a σ_u one, it nevertheless reflects the initial state symmetry, thus allowing one to test the hypothesis that the symmetry of the initially occupied orbital is decisive. The electron-electron interaction which mediates the transition is assumed to be a contact interaction. With these approximations, g_2 reads explicitly:

$$g_{2,\pm} = \frac{h_{2,\pm}(|\mathbf{R}|)}{2|E_2| + (\mathbf{k} - \mathbf{p}_1 - \mathbf{p}_2)^2} \begin{cases} \cos\frac{(\mathbf{k}-\mathbf{p}_1-\mathbf{p}_2)\cdot\mathbf{R}}{2} & (+) \\ \sin\frac{(\mathbf{k}-\mathbf{p}_1-\mathbf{p}_2)\cdot\mathbf{R}}{2} & (-), \end{cases} \tag{1}$$

where $h_{2,\pm}$ is a function of the internuclear separation $|\mathbf{R}|$. It is not relevant for the further discussion. $|E_2|$ is the time dependent ionization potential of the singly charged ion [23].

The transition matrix element of the first electron to the continuum is split into a rate part and into g_1, a geometry part, which is incorporated in the form factor. The orbital initially occupied by the electron is again constructed using the LCAO method as above and, consequently, a contact electron-ion interaction is used. g_1 then appears as an intermediate state interference term:

$$g_{1,\pm} = h_{1,\pm}(|\mathbf{R}|) \begin{cases} \cos\frac{\mathbf{k}\cdot\mathbf{R}}{2} & (+) \\ \sin\frac{\mathbf{k}\cdot\mathbf{R}}{2} & (-). \end{cases} \tag{2}$$

In Eqs. (1) and (2), the $(+)$ is for the σ_g and the $(-)$ for the σ_u initially occupied orbital. In terms of g_1 and g_2, the model form factor reads $|V_{\mathbf{p}_1, \mathbf{p}_2, \mathbf{k}}|^2 = |g_1(\mathbf{k})g_2(\mathbf{p}_1, \mathbf{p}_2, \mathbf{k})|^2$. Again we average over the random orientation of the internuclear axis.

The calculated electron momentum correlations for $p_{i,\parallel}$, $i = 1, 2$ are shown in Fig. 2(c) for N_2 and in Fig. 2(d) for O_2. For N_2, we find a correlation qualitatively similar to that observed in the experiment with a significant amount of events appearing where both electrons have small and similar $p_{i,\parallel}$, $i = 1, 2$. The calculation indicates that the specific shape of the distribution is mainly determined by final state interference via the matrix element $g_{2,+}$. Changing $g_{1,+}$ (e.g., using its atomic value 1) has only little effect. The reason for this is that $\mathbf{k}\mathbf{R}/2 < \pi/2$ [with $\mathbf{k} = -\mathbf{A}(t')/c$, t': transition time of the first electron to the continuum], where the first zero of

$g_{1,+}$ appears. An increasing influence of $g_{1,+}(\mathbf{k})$, is expected at light intensities where $\mathbf{k}\mathbf{R}/2 > \pi/2$.

O_2 shows a significantly different correlation [Fig. 2(d)]. In spite of the slightly higher light intensity, it is concentrated near $p_{1,\|} = p_{2,\|} = 0$. This again is similar to what is found in the experiment [Fig. 2(b)] together with a correspondingly narrow electron sum-momentum distribution [light gray line in Fig. 1(c)]. The good agreement between experiment and model calculation does not persist with increasing light intensity as one may expect from the simple model. The experimental width of the sum-momentum distribution slowly increases with $2\sqrt{U_p}$ while the model gives rise to a slightly decreasing width. At the lowest light intensity investigated [Fig. 1(b)], the qualitative agreement is lost. In contrast to the experiment, the calculated electron momentum correlation develops a double hump structure. This discrepancy probably has its origin in our classical approach. The classically accessible phase space where $E_{\mathrm{kin}}(t) \geq |E_2(t)|$ [23] gets very small around $p_{i,\|} = 0$. Quantum mechanics may remove this discrepancy. The origin of the localized electron momentum correlation for O_2 [Fig. 2(d)] is found in $g_{1,-}$. The sine term suppresses recollision of electrons with small $\mathbf{k}$ which are field ionized near the extrema of the oscillating electric field. This in turn leads to an efficient suppression of final state electrons with large $p_{i,\|}$. At low light intensity, the influence of this term is found to be reduced significantly. Different from N_2, the initial state symmetry thus comes in mainly via $g_{1,-}$.

In conclusion, we have provided evidence for NSDI of N_2 and O_2. The main features found can be understood within the framework of the recollision model with direct electron impact ionization of the singly charged molecular ion. But molecular structure decisively influences the electron momentum correlation. In fact, it appears to be more important than for single ionization. For N_2 molecular structure mainly affects the inelastic recollision. This gives rise to distinct differences between N_2 and Ar correlation spectra. On the other hand, the momentum correlation for O_2 is mainly determined by the transition matrix element to the continuum [Eq. (2)] of the electron ionized first. The main influence of molecular structure is found in the electron sum momentum (main diagonals in Fig. 2). The effect on the difference momentum (minor diagonals in Fig. 2) is less pronounced. Averaging over statistically oriented molecular axes in the experiment and calculation washes out much of the interference that is due to molecular structure. The model calculation shows that aligning the axis should give rise to a much more pronounced effect.

We gratefully acknowledge very enlightening discussions with Andreas Becker and Wilhelm Becker. The work was supported by the Deutsche Forschungsgemeinschaft (DFG) and by the Welch Foundation.

[1] A. l'Huillier, L. A. Lompre, G. Mainfray, and C. Manus, Phys. Rev. A **27**, 2503 (1983); D. N. Fittinghoff, P. R. Bolton, B. Chang, and K. C. Kulander, Phys. Rev. Lett. **69**, 2642 (1992); B. Walker *et al.*, Phys. Rev. Lett. **73**, 1227 (1994).

[2] P. B. Corkum, Phys. Rev. Lett. **71**, 1994 (1993); K. C. Kulander, J. Cooper, and K. J. Schafer, Phys. Rev. A **51**, 561 (1995).

[3] K. Kondo, A. Sagisaka, T. Tamida, Y. Nabekawa, and S. Watanabe, Phys. Rev. A **48**, R2531 (1993); D. N. Fittinghoff, P. R. Bolton, B. Chang, and K. C. Kulander, Phys. Rev. A **49**, 2174 (1994); P. Dietrich, N. H. Burnett, M. Ivanov, and P. B. Corkum, Phys. Rev. A **50**, R3585 (1994).

[4] Th. Weber *et al.*, Phys. Rev. Lett. **84**, 443, (2000).

[5] R. Moshammer *et al.*, Phys. Rev. Lett. **84**, 447 (2000).

[6] Th. Weber *et al.*, Nature (London) **405**, 658 (2000).

[7] B. Feuerstein *et al.*, Phys. Rev. Lett. **87**, 043003 (2001).

[8] C. Cornaggia and Ph. Hering, J. Phys. B **31**, L503 (1998).

[9] C. Guo, M. Li, J. P. Nibarger, and G. N. Gibson, Phys. Rev. A **58**, R4271 (1998).

[10] C. Cornaggia and Ph. Hering, Phys. Rev. A **62**, 023403 (2000).

[11] C. Guo and G. N. Gibson, Phys. Rev. A **63**, 040701 (2001).

[12] Hiromichi Niikura *et al.*, Nature (London) **417**, 917 (2002).

[13] A. S. Alnaser *et al.*, Phys. Rev. Lett. **91**, 163002 (2003).

[14] F. Grasbon *et al.*, Phys. Rev. A **63**, 041402 (2001).

[15] A. Talebpour, C.-Y. Chien, and S. L. Chin, J. Phys. B **29**, L677 (1996).

[16] J. Muth-Böhm, A. Becker, and F. H. M. Faisal, Phys. Rev. Lett. **85**, 2280 (2000).

[17] Also, a charge-screening correction to tunnel ionization was suggested to explain the phenomenon [18]. Recent experimental data even seem to indicate that neither charge-screening nor initial state orbital symmetry is sufficient to quantitatively predict single ionization of diatomics in general [19].

[18] C. Guo, Phys. Rev. Lett. **85**, 2276 (2000).

[19] M. J. DeWitt, E. Wells, and R. R. Jones, Phys. Rev. Lett. **87**, 153001 (2001).

[20] R.W. Wetmore and R. K. Boyd, J. Phys. Chem. **90**, 5540 (1986); M. Larsson *et al.*, J. Phys. B **23**, 1175 (1990).

[21] J. Ullrich *et al.*, J. Phys. B **30**, 2917 (1997).

[22] R. Moshammer *et al.*, Opt. Express **8**, 358 (2001).

[23] E. Eremina *et al.*, J. Phys. B **36**, 3269 (2003).

[24] C. Guo, M. Li, J. P. Nibarger, and G. N. Gibson, Phys. Rev. A **61**, 033413 (2000).

[25] F. Lindner, G. G. Paulus, F. Grasbon, A. Dreischuh, and H. Walther, IEEE J. Quantum Electron. **38**, 1465 (2002).

[26] R. Moshammer *et al.*, J. Phys. B **36**, L113 (2003).

[27] M. B. Smirnov and V. P. Krainov, Zh. Eksp. Teor. Fiz. **113**, 583 (1998) [J. Exp. Theor. Phys. **86**, 323 (1998)]; M. B. Smirnov and V. P. Krainov, Phys. Scr. **57**, 420 (1998).

[28] C. Figueira de Morisson Faria, X. Liu, W. Becker, and H. Schomerus, Phys. Rev. A **69**, 021402 (2004).

[29] S. P. Goreslavski, S.V. Propruzhenko, R. Kopold, and W. Becker, Phys. Rev. A **64**, 053402 (2001).